Antiviral Research 164 (2019) 61–69

Contents lists available at ScienceDirect

Antiviral Research

journal homepage: www.elsevier.com/locate/antiviral

Human cathelicidin peptide LL-37 as a therapeutic antiviral targeting Venezuelan equine encephalitis virus infections

Aslaa Ahmed[a], Gavriella Siman-Tov[a], Forrest Keck[a], Stephanie Kortchak[a], Allison Bakovic[a], Kenneth Risner[a], Timothy K. Lu[b,c,d], Nishank Bhalla[a], Cesar de la Fuente-Nunez[b,c,d,*], Aarthi Narayanan[a,**]

[a] National Center for Biodefense and Infectious Disease, School of Systems Biology, George Mason University, Manassas, VA, USA
[b] Synthetic Biology Group, MIT Synthetic Biology Center; The Center for Microbiome Informatics and Therapeutics; Research Laboratory of Electronics, Department of Biological Engineering, Cambridge, MA, USA
[c] Department of Electrical Engineering and Computer Science, Massachusetts Institute of Technology, Cambridge, MA, USA
[d] Broad Institute of MIT and Harvard, Cambridge, MA, USA

ARTICLE INFO

Keywords:
Venezuelan equine encephalitis virus
Antimicrobial peptides
Cathelicidins
LL-37
IFN- β
Antivirals

ABSTRACT

Venezuelan equine encephalitis virus (VEEV), a new world alphavirus belonging to the *Togaviridae* family, causes periodic disease outbreaks in humans and equines with high associated mortality and morbidity. VEEV is highly infectious via the aerosol route and so has been developed as a biological weapon (Hawley and Eitzen, 2001). Despite its current classification as a category B select agent, there are no FDA approved vaccines or therapeutics to counter VEEV infections. Here we utilize a naturally occurring host defense peptide, LL-37, as a therapeutic strategy to inhibit VEEV multiplication in infected cells. LL-37 has previously demonstrated activity against several viruses by directly interacting with viral particles and indirectly by establishing an antiviral state in the host cell. We show that LL-37 exhibited potent antiviral activity against VEEV by inhibiting viral replication. Genomic RNA copies of the TC-83 strain of VEEV and viral titers were significantly reduced compared to non-treated controls. LL-37 also inhibited the virulent Trinidad Donkey (TrD) strain of VEEV. Entry assays revealed a robust reduction of viral RNA copies at the early stages of TC-83 infection. Pre-incubation of cells with LL-37 and TC-83 resulted in a strong inhibitory response, indicating that LL-37 impacts early stages of the infectious process. Confocal and electron microscopy images confirmed the aggregation of viral particles, which potentially accounts for entry prevention and hence reduced viral infection. LL-37 treatment also modulated type I interferon (IFN) expression in infected cells. LL-37 treatment dramatically increased IFNβ1 expression in treated cells in a time-dependent manner. Our results establish LL-37 as a relevant and novel potential therapeutic strategy for the treatment of VEEV infections.

1. Introduction

Venezuelan equine encephalitis virus (VEEV) is an arbovirus that causes periodic outbreaks in the Americas, resulting in febrile and neurological illnesses. Spreading over large geographical regions, VEEV outbreaks affect thousands of humans and equines (Weaver et al., 2004). VEEV is an enveloped, positive-sense RNA virus with a genome approximately 11.4 kb in length (Paessler and Weaver, 2009; Strauss and Strauss, 1994). Two-thirds of the 5'end of the genome codes for four nonstructural proteins (nsp1-4) that are required for replication, while the 3′ end codes for structural proteins (Paessler and Weaver, 2009). VEEV has been previously characterized as a category B select agent because of its ease of aerosolization and retention of infectivity in aerosol form. VEEV infections manifest with flu-like symptoms, including high fever, headaches, and malaise. While the fatality rate is < 1%, encephalitic cases are more serious with a fatality rate as high as 20% and the potential development of permanent neurological sequelae (Cain et al., 2017; Weaver et al., 2004). Neuronal cells are highly susceptible to VEEV infections; high viral dissemination leads to neuroinflammation and loss of blood-brain barrier integrity (Cain et al.,

* Corresponding author. Synthetic Biology Group, MIT Synthetic Biology Center; The Center for Microbiome Informatics and Therapeutics; Research Laboratory of Electronics, Department of Biological Engineering, Cambridge, MA, USA.
** Corresponding author.
E-mail address: cfuente@mit.edu (C. de la Fuente-Nunez).

https://doi.org/10.1016/j.antiviral.2019.02.002
Received 12 November 2018; Received in revised form 20 January 2019; Accepted 3 February 2019
Available online 08 February 2019
0166-3542/

2017). Currently, there are no FDA-approved treatments or vaccines targeting VEEV.

Antimicrobial peptides (AMPs), also known as host defense peptides, are a crucial component of innate immunity (Brown and Hancock, 2006). These oligopeptides comprise a few to over a hundred amino acids (Bahar and Ren, 2013). In humans, there are two major classes of host defense peptides, defensins and cathelicidins. LL-37, the sole human peptide of the cathelicidin family, is a cationic peptide encoded by the CAMP gene, which is expressed in numerous cell types, including neutrophils, macrophages, and endothelial cells (Durr et al., 2006). The peptide is present as an inactive precursor molecule stored in neutrophils; its biological effects are activated upon proteolytic cleavage (Durr et al., 2006). LL-37 has been studied for use as an alternative to antibiotics for microbial infections. The inhibitory effects of this peptide have been attributed to its direct antimicrobial killing properties (Brown and Hancock, 2006). Recently, research on LL-37 has demonstrated activity against a multitude of viruses. Susceptible enveloped viruses include: influenza type A virus (IVA), human immunodeficiency virus (HIV), Zika virus (ZIKV), dengue type-2 virus (DENV-2), hepatitis C virus (HCV), and vaccinia virus (Alagarasu et al., 2017; Barlow et al., 2011; Bergman et al., 2007; He et al., 2018; Howell et al., 2004; Matsumura et al., 2016; Steinstraesser et al., 2005; Tripathi et al., 2013). In addition, LL-37 modifies and activates immune responses by promoting the recruitment of immune cells and modulating the inflammatory response (Brown and Hancock, 2006), effects that have also been observed with synthetic peptides (de la Fuente-Nunez et al., 2014; Silva et al., 2016).

In this study we assessed the antiviral activity of LL-37 against VEEV. We utilized the TC-83 strain of VEEV to demonstrate the activity of LL-37 in multiple neuronal cell lines. We detected a significant decrease in viral replication 16-hours post-infection (hpi) as depicted by quantified viral titers. The measurement of genomic TC-83 copies confirmed the decrease in viral replication. We also determined that LL-37 exerted a robust inhibitory activity against the virulent Trinidad Donkey (TrD) strain of VEEV. To determine the mechanism of action of LL-37, we assayed viral RNA copies at an early time point during the course of infection, which revealed the peptide to function as an entry inhibitor. We further explored the impact of peptide treatment on viral infection by employing transmission electron microscopy (TEM) and immunofluorescence. To further determine post-entry effects of LL-37 treatment, we analyzed inflammatory modulation by assessing the expression of interferons (IFNs) and determined that LL-37 induces IFNβ1 expression. Collectively, our data suggest that LL-37 inhibits VEEV multiplication by direct mechanisms that impair the virus and indirect mechanisms that influence the establishment of an antiviral state in the host cell.

2. Materials and Methods

2.1. Cell culture and reagents

Mouse brain microglia (BV2, EOC 20 CRL-2469), human astrocytoma (U87MG, HTB-14), and human microglia (HMC3, CRL-3304) cell lines were all acquired from American Type Culture Collection, Manassas, VA. BV2 and U87MG cells were maintained in Dulbecco's Modified Eagle's Medium (DMEM) supplemented with 1% L-glutamine, and 1% penicillin/streptomycin and heat-inactivated Fetal Bovine Serum (FBS) at 5% and 10%, respectively. HMC3 was maintained in Eagle's Minimum Essential Medium supplemented with 1% penicillin/streptomycin and 10% FBS. Vero cells (ATCC, CCL-81) were maintained in DMEM supplemented with 5% FB Essence (VWR, 10799-390P), 1% penicillin/streptomycin, and 1% L-glutamine. All cell cultures were maintained at 37 °C with 5% CO_2. LL-37 (LLGDFFRKSKEKIGKEFKRIVQRIKDFLRNLVPRTES) was obtained from Peptide Sciences, USA, and reconstituted with ultrapure water to a final stock concentration of 1 mg/mL. The scrambled LL-37 (GLKLRFEFSKIKGEFLKTPEVRFRDIKLKDNRISVQR) control was acquired from AnaSpec, Fremont, CA. Both peptides were purified by high performance liquid chromatography (HPLC) with > 95% purity.

2.2. Viruses and infections

VEEV TC-83 was obtained from BEI Resources. TC-83 is a result of 83 passages of the fully virulent IAK Trinidad donkey (TrD) strain (Kinney et al., 1989). TC-83 is a well-established BSL-2 VEEV model for the TrD strain for which replication has been well studied *in vitro* and *in vivo* (Kehn-Hall et al., 2012). The attenuation associated with TC-83 was mapped to the changes in the 5′-noncoding region and the E2 envelope glycoprotein (Kehn-Hall et al., 2012). Experiments with TC-83 were performed under BSL-2 while those with TrD were performed under BSL-3 requirements and procedures.

For all infections, cells were seeded in 96-well plates and allowed to reach confluency for approximately 24 h prior to infection. Upon confluency, cells were either 1) pre-treated (pLL-37) with the appropriate concentration of LL-37 for two hours to allow for peptide internalization, infected with virus at the desired multiplicity of infection (MOI), and incubated at 37 °C for 1 h to allow for viral absorption; or 2) treated with the appropriate concentration of LL-37, then immediately infected with virus at the desired multiplicity of infection (MOI), and incubated at 37 °C for 1 h to allow for viral absorption. For entry assays, TC-83 at different MOIs was pre-incubated with LL-37 for 30 min at 37 °C prior to infection (pre-incLL-37). The pre-incubated inoculum was used to infect cells. The viral inoculum was removed and replaced with peptide-only media to allow for constant exposure to peptide. The cells were incubated at 37 °C, 5% CO_2 for 3 h for entry assays and 16 h for all other infections. Supernatants were collected after incubation and either stored at −80 °C until analyzed or processed upon collection.

2.3. Cell viability assays

Cell viability was measured using CellTiter-Glo Luminescent Cell Viability Assay (Promega, G7572) per the manufacturer's instructions. Cells were seeded at a density of 1E4 cells/mL and grown until confluency. The cells were treated with either LL-37 or the scrambled control at various concentrations for an additional 24 h. Cell viability was determined by the addition of the CellTiter-Glo reagent to cells at a ratio of 1:1. The plate was placed on a plate shaker for 2 min followed by a 10-min incubation at room temperature. Cell viability was measured as luminescence detected using the DTX 880 multimode detector (Beckman Coulter). Percent viability was normalized to water-only treatment, as water served both as a control and as the LL-37 carrier to avoid osmotic shock to the cells.

2.4. Plaque assay

Plaque assays were performed as described in Baer and Kehn-Hall (2014) (Baer and Kehn-Hall, 2014). Vero cells were seeded in 12-well plates at a density of 2.5E5 cells/mL. The cells were grown overnight at 37 °C, 5% CO_2 until confluent. Viral supernatants were serially diluted in DMEM in deep well plates and used to infect Veros. All plates were incubated at 37 °C, 5% CO_2 for 1 h with rocking in 15-min intervals. An overlay consisting of 2X E-MEM and 0.06% agarose at 1:1 ratio was added to each well. Upon solidification of the overlay, the plates were incubated for an additional 48 h at 37 °C. The cells were fixed using 1 mL of a 10% formaldehyde solution added to the surface of the plugs for 1 h at room temperature. The plates were rinsed with diH20 to remove the plugs. A solution of 1% crystal violet, 20% ethanol was used to stain the plates. The plates were rinsed with diH20 and plaques were counted to determine viral titers as plaque forming units (PFU/mL).

2.5. Quantitative RT-PCR (qRT-PCR)

Cells were treated with LL-37 at a non-toxic concentration, as determined by viability assay, and infected with TC-83 at an MOI of 0.1 or at MOIs of 0.1, 1, and 5 for entry assays. Cells were lysed and intracellular and extracellular RNAs were extracted using Qiagen RNeasy and QIAamp Viral RNA mini kits, respectively, per the manufacturer's protocol (Qiagen, 74104 and 52906). The pre-cycling conditions were adapted from Verso 1-step RT-qPCR kit (ThermoFisher AB4101C) manufacturer's instructions: 1 cycle at 50 °C for 20 min, 1 cycle at 95 °C for 15 min, 40 cycles at 95 °C for 15 s and at 51 °C for 1 min using StepOnePlus™ Real Time PCR system. Primers and probes for VEEV TC-83 targeted nucleotides 7931-8005, which encode the capsid, as originally described by Julander et al. (2008): forward primer (TCTGA CAAGACGTTCCCAATCA) and reverse primer (GAATAACTTCCCTCCG ACCACA) (Julander et al., 2008). However, the probe utilized different tags (5′6-FAM/TGTTGGAAG/ZEN/GGAAGATAAACGGCTACGC/ 3′IABkFQ) to improve sensitivity. The nsp2 primers/probes are as follows: forward primer (CCT CTC GCT GAA CAA GTC ATA G), reverse primer (CCT CTG GCA CCA CTA CTT TAC) and probe (/56-FAM/TG GTA TGG T/Zen/T CCA CGG CAT AAC GC/3IABkFQ/). Both sets were designed by and obtained from Integrated DNA Technologies (Skokie, Il). Quantification was calculated by standard curve based on threshold cycle (Ct). For Taqman expression assays, cells were lysed using 300 µL TRIzol reagent, and RNA was extracted using Zymo Direct-zol RNA Miniprep kit (Zymo Research, R2050) as per the manufacturer's protocol. The total RNA was converted to cDNA using the High-Capacity RNA-to-cDNA reverse transcription kit (ThermoFisher, 438814). Expression was determined using the ΔΔCt method with ThermoFisher Taqman reagents for CAMP/LL-37 (Hs01011708-m1), IFNB1 (Hs01077958-s1), IFNG (Hs00989291-m1), and 18S RNA (HS99999901-s1).

2.6. Immunofluorescence

HMC3 cells were seeded in an 8-well chambered slide (ibidi, 80841) at a density of 1E4 cells/mL. Cells were either mock treated or LL-37 treated and infected at MOI of 5, as described above for entry assays. Cells were fixed with 4% paraformaldehyde for 10 min at room temperature and permeabilized with 0.1% Triton X-100 for 10 min. The cells were subsequently washed with PBS and blocked at room temperature with 1% BSA for 30 min. The cells were incubated with primary antibody to TC-83 glycoprotein in 1% blocking solution overnight at 4 °C. A secondary antibody specific to the primary antibody was added to the cells in blocking buffer for 1 h in the dark at room temperature. The cells were washed with PBS, treated with Hoechst dye (ThermoFisher, 33342), and incubated for 15 min at room temperature. An additional PBS wash was performed followed by mounting the slides with 2 drops of ibidi mounting medium and storing them in the dark. Images were taken at 60× magnification using Nikon Eclipse TE2000-U.

2.7. TEM

TEM was performed on HMC3 cells at 3hpi. Cells were seeded at a density of 3E5 cells/mL in 6-well plates. Cells were treated with LL-37 and infected at an MOI of 5 as described above for the entry assays. Samples were fixed with 2.5% glutaraldehyde, 1% paraformaldehyde in 0.12 M sodium cacodylate buffer and pelleted. The cell pellets were enrobed in low melting point agarose. Cells were post-fixed with 1% osmium tetroxide and 1% uranyl acetate. After a series of ethanol dehydrations, the cells were embedded in Embed812 resin and cured for 2 days at 60 °C. The resin blocks were sectioned to a thickness of 70 nm on a Leica Ultracut EM UC7 Ultramicrotome. Sections were post-stained with uranyl acetate and lead citrate and then imaged using Talos F200X TEM (ThermoFisher Scientific).

2.8. Statistical analysis

All images and statistical analyses were acquired using Graph Pad Prism software version 7. Replicate numbers are as specified in figure legends. Results were analyzed by unpaired one-way ANOVA test. Data are presented as a mean with ± SD. Statistical significance is indicated as follows: *$p < 0.05$; **$p < 0.01$; ***$p < 0.001$; ****$p < 0.0001$.

3. Results

3.1. LL-37 inhibits TC-83 replication in multiple cell lines

LL-37 has been shown to be a potent antiviral molecule, as evidenced by its inhibition of the replication of many viruses, including IAV, HIV, ZIKV, and DENV-2, (Alagarasu et al., 2017; Bergman et al., 2007; He et al., 2018; Tripathi et al., 2013). As a first step to evaluating the inhibitory potential of LL-37 against VEEV in a cell type-independent manner, we established the baseline replication kinetics of the TC-83 strain of VEEV in three model cell lines, namely BV2 cells (murine), U87MG cells (human astroglioma cells), and HMC3 cells (human microglial cells). The cell lines were infected with TC-83 and titers were quantified at 16 hpi as infectious PFUs and genomic TC-83 copies (Fig. 1 A and B). Cell viability for all cell lines following treatment with LL-37 or the scrambled control peptide was measured at increasing concentrations of peptide (10, 50, and 100 µg/mL). LL-37 was nontoxic at a concentration of up to 50 µg/mL whereas the scrambled control was nontoxic even at 100 µg/mL (Fig. 1 C). Infectious TC-83 titers were measured following treatment with LL-37 (10 µg/mL) in the BV2 murine cell line as a first proof-of-concept investigation, which demonstrated a decrease in viral titer of about 100-folds (Fig. 1 D). The cells were subjected to two treatment conditions: 1) cells were pretreated with LL-37 for 2 h prior to infection (preLL-37), and 2) LL-37 treatment was administered at the time of TC-83 infection (LL-37), i.e., without pretreatment (see Materials and Methods).

The purpose of using the two conditions was to assess the effect of LL-37 pretreatment on viral replication. While the TC-83 titer decreased in both conditions (pretreated and non-pretreated cells), preLL-37 produced a slightly higher titer (less of a decrease). This difference was possibly a result of LL-37 internalization during pretreatment, hence decreasing the concentration of peptide available to interact with the virus. The scrambled control, unlike LL-37, demonstrated no inhibitory effects, thus supporting the specificity of inhibition observed with LL-37 treatment. At 16 hpi, extracellular copies of the TC-83 RNA genome were extracted from supernatants and quantified by qRT-PCR. Consistent with the plaque assay results, LL-37 caused a 100-fold decrease in TC-83 genomic copies as compared to controls, indicating an inhibition of viral replication (Fig. 1 E).

3.2. LL-37 inhibition is not cell type-dependent

To determine whether the inhibition demonstrated by LL-37 in BV2 cells is a cell type-dependent phenomenon, we tested the peptide in human microglia and astrocyte cell lines. Cell viability in both cell lines was determined using the above-mentioned concentrations of LL-37 (Fig. 2). We used the highest tolerated concentration of peptide for infections (U87MG = 50 µg/mL; HMC3 = 10 µg/mL). Plaque assays indicated that the inhibitory effects of LL-37 were, indeed, not cell type-dependent, as LL-37 caused an approximate 100-fold decrease as compared to the water-only control in both cell types (Fig. 2 C and D). The scrambled peptide control partially inhibited TC-83 replication in both cell lines; however, this inhibition was less robust than that observed with LL-37 and was not significant. When we tested the effect of LL-37 on the fully virulent TrD strain, we observed a very robust inhibition of virus with LL-37 treatment (Fig. 2 E).

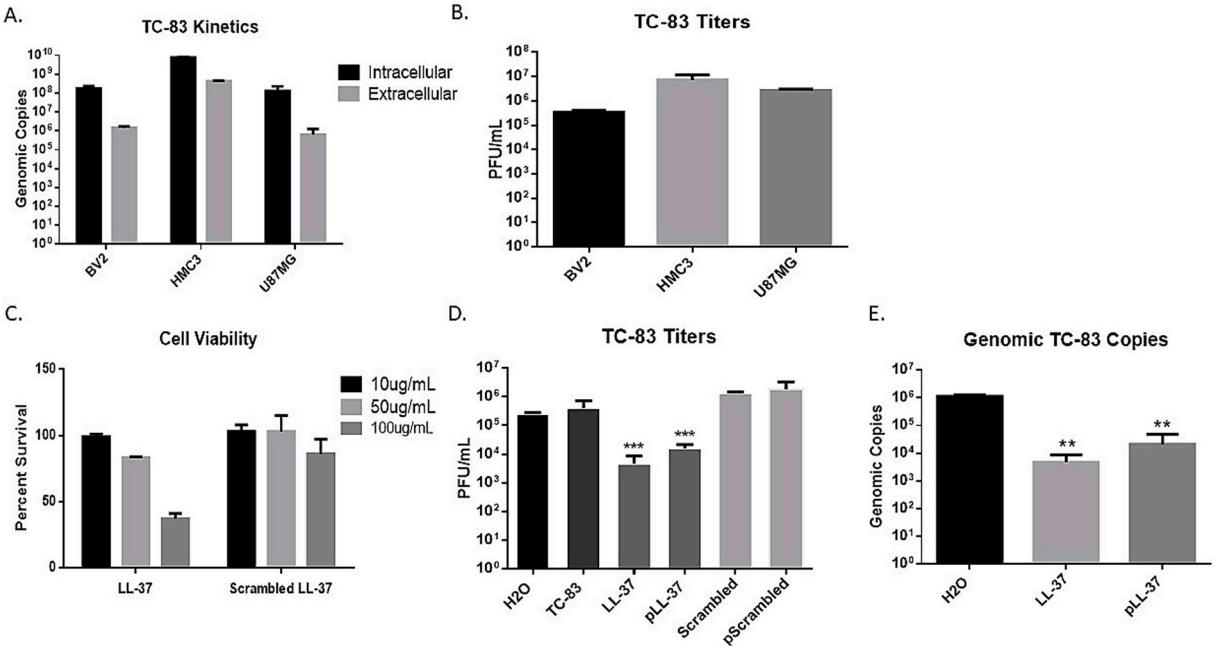

Fig. 1. Toxicity and inhibitory efficacy of LL-37. (A and B) Replication kinetics of TC-83 in cell lines BV2, HMC3, and U87MG. (C) BV2 cells were treated with diluted LL-37 or scrambled LL-37 to determine toxicity. Luminescence was measured using Cell Titer-Glo at 24 h post treatment and reported as a percentage normalized to the water-only control. (D) A plaque assay was used to determine titers of TC-83 under LL-37 (10 μg/mL) treatment using scrambled LL-37 (50 μg/mL) as a control in addition to a water-only control. pLL-37/pScrambled represents cells pre-treated with each peptide; LL-37/Scrambled represents cells with no pretreatment, i.e., peptides and virus were added at the same time. (E) Copies of the TC-83 RNA genome were measured using qRT-PCR (see Materials and Methods). All infections were done at an MOI of 0.1. Statistical analysis is in comparison to the water-only control. Data represents means ± SD (n = 3). **p < 0.01, ***p < 0.001.

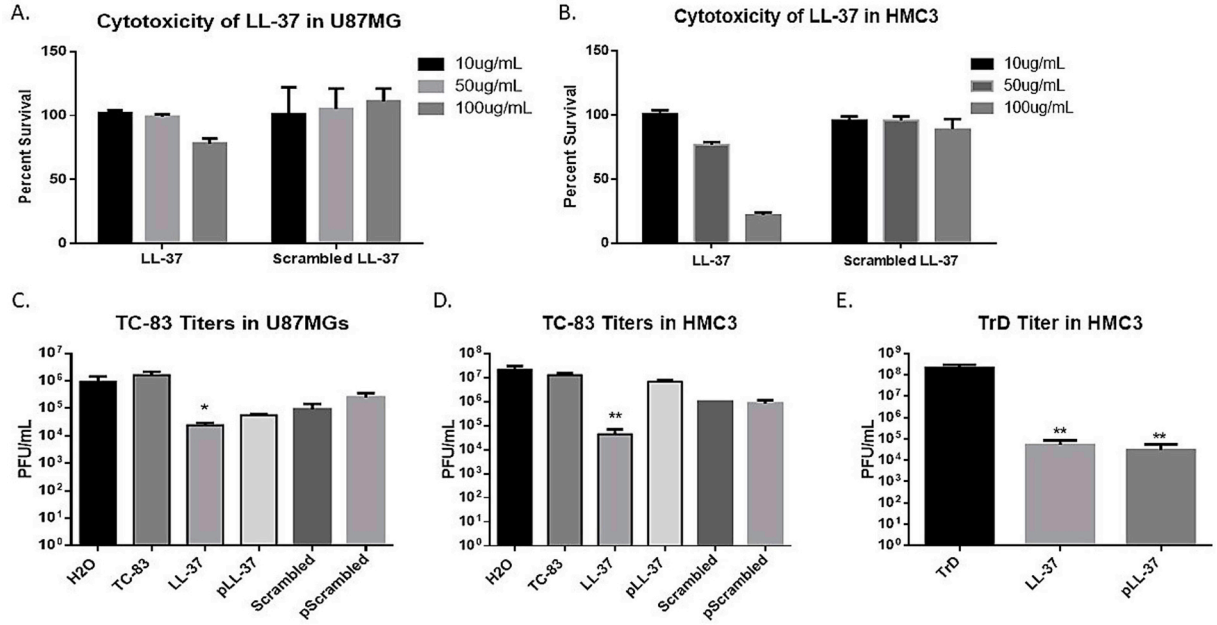

Fig. 2. Toxicity and efficacy of LL-37 in HMC3 and U87MG cells. (A and B) Cytotoxicity was determined using Cell Titer-Glo by incubating the cells for 24 h with LL-37 or scrambled LL-37 at various concentrations. Cell viability is reported as a percentage of live cells normalized to cells treated with water only. (C and D) Titers of TC-83 in HMC3 and U87MG cells as determined by plaque assay. Concentrations of LL-37 for HMC3 and U87MG cells, obtained from the viability assay, were 10 μg/mL and 50 μg/mL, respectively, and concentration of the scrambled peptide control for both cell lines was 50 μg/mL. (E) Titers of the virulent VEEV strain, TrD, in HMC3 cells using 10 μg/mL of LL-37. All infections were performed at an MOI of 0.1 for 1 h, and supernatants were collect at 16 hpi. pLL-37/pScrambled represents cells pretreated with LL-37 or scrambled peptide. Statistical analysis is in comparison to water-only control. Data reported as mean ± SD (n = 3). *p < 0.05, **p < 0.01.

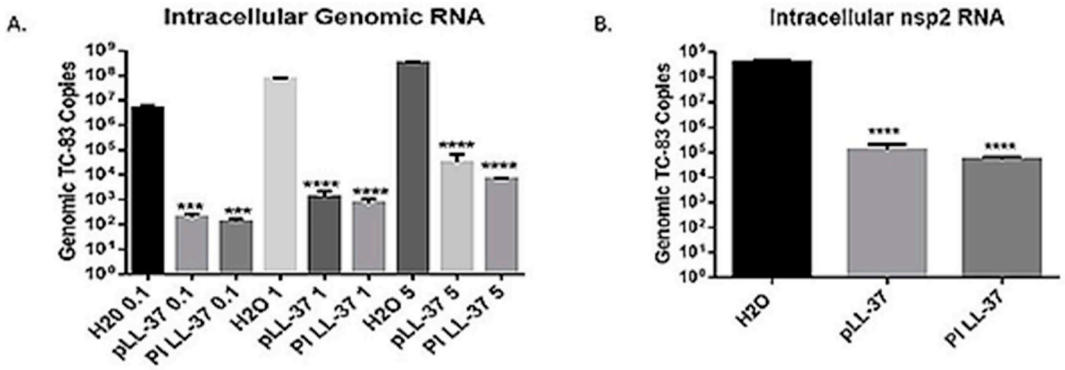

Fig. 3. Entry inhibition of VEEV following LL-37 treatment. (A) Cells were treated with LL-37 at 10 μg/mL and infected with TC-83 for 1 h at MOIs of 0.1, 1, and 5. Total intracellular RNA was extracted and quantified using qRT-PCR at 3 hpi (see Materials and Methods). Primers targeting VEEV capsid protein were utilized. (B) Intracellular RNA for cells infected at an MOI of 5 was quantified using primers for VEEV nsp2. VEEV RNA was quantified using qRT-PCR. pLL-37 represents cells pre-treated with LL-37; PI LL-37 represents cells infected with TC-83 that was pre-incubated with LL-37. Data reported as mean ± SD (n = 3). ***p < 0.001, ****p < 0.0001.

3.3. The early stages of TC-83 infection cycle are susceptible to LL-37 treatment

LL-37 has been demonstrated to directly inhibit the early stages of infection for several viruses, particularly when treatment is administered prior to infection or when virus and peptide are pre-incubated prior to infection. This mechanism of inhibition has been documented for IAV, HIV, DENV-2, and HCV (Alagarasu et al., 2017; Bergman et al., 2007; Matsumura et al., 2016; Tripathi et al., 2013). To determine whether LL-37 acts as an inhibitor of early VEEV infection events, we looked at TC-83 genomic copies at an early post-infection time point. Using three MOIs (0.1, 1, and 5), we infected HMC3 cells either with TC-83 in LL-37, or with TC-83 that had been pre-incubated with LL-37 for 30 min. After incubation for 1 h at 37 °C, the viral inocula were removed and cells were washed three times with PBS to remove any residual extracellular virus. Peptide-treated media was added back to the appropriate cells, and cells were lysed at 3 hpi to quantify intracellular copies of the TC-83 genome. At 3 hpi, for all MOIs, there were significantly fewer intracellular copies of the TC-83 genome compared to the number of copies in the water-only control (Fig. 3 A). These results indicated that LL-37 impacts the early processes of TC-83 infection. To further validate the data, we used nsp2 primers, corresponding to sequences encoding nonstructural proteins of the viral genome, to quantify the genomic copies of TC-83 at an MOI of 5. The results confirmed a significant decrease in the number of viral genomic copies as compared to those in the water-only control (Fig. 3 B).

3.4. LL-37 sequesters TC-83 extracellularly and intracellularly in the form of clumps

LL-37 has been extensively studied in terms of binding to and interfering with virus outer membrane moieties (Howell et al., 2004; Matsumura et al., 2016). *In silico* analysis and molecular docking studies revealed the binding of LL-37 to the viral envelope of DENV-2 as a mechanism of viral entry inhibition (Alagarasu et al., 2017). Not only does LL-37 interfere with membranes of enveloped viruses, it has also been shown to disrupt non-enveloped viruses. Electron microscopy images of LL-37/vaccinia interactions demonstrate loss of integrity of the external envelope and internal structures (Howell et al., 2004). To assess the interaction of LL-37 and TC-83 and to help visualize the effect of LL-37 on the virus, we performed immunofluorescence studies. Using fluorescent antibodies, we observed clumping of TC-83 in the vicinity of LL-37-treated cells. The images obtained were of cells infected at an MOI of 5 and were taken at 0.5 hpi, an early time point during infection. The images demonstrated clumping of viruses throughout the LL-37-treated cells (Fig. 4). This trend can be seen for both pre-treatment and pre-incubation with LL-37; however, while there was no apparent localization of these clumps in terms of the extracellular vs. the intracellular environment in pre-incLL-37-treated cells, in preLL-37 samples clumping or viral aggregation was more evident extracellularly. In cells treated with the scrambled peptide control, the virus seemed to be more evenly distributed throughout the cell and clumps were absent.

To further validate our hypothesis that LL-37 treatment impacts viral entry, we obtained TEM images at 3 hpi from cells that were infected with TC-83 at an MOI of 5. While intact whole virions were visualized in the untreated control group, no whole virions were detected in the LL-37-treated groups (Fig. 4). Consistent with LL-37 treatment, there was also a lack of whole virions in the LL-37/TC-83 pre-incubation condition (pre-incLL-37, Fig. 5). Extracellular images portrayed a dense cluster of what could possibly be LL-37 viral clumps in the LL-37 treated cells (Fig. 5 A). Intracellular images revealed the presence, in the water-only control groups, of virions within what appear to be vesicles (Fig. 5 B). However, in the LL-37 treated cells, vesicles containing a cluster of dense matter can be seen throughout the cells (Fig. 5). While the viral clumps can be seen both intracellularly and extracellularly, the intensity of the clusters in the extracellular environment was much higher, potentially leading to the observed mechanism of action of LL-37 preventing viral entry. Consistent with previous results, these images provide data to support the direct interaction of LL-37 with viral particles.

3.5. LL-37 modulates type 1 interferon expression

LL-37 not only directly inhibits multiple viruses; it has also been shown to exhibit immune modulatory activities (Agier et al., 2015). Interferons (IFNs) are an important component of the innate immune antiviral response. LL-37 has been previously demonstrated to inhibit IFN-ϒ responses (Nijnik et al., 2009). In addition, IFN-β expression levels were significantly decreased in ZIKV-infected astrocytes treated with an AMP comprising the major antimicrobial region of LL-37 (He et al., 2018). We aimed to determine the effect LL-37 exerts on IFN expression and thereby on the innate immune response, for uninfected cells and for cells infected with TC-83. We utilized Taqman expression assays to assess the effect exogenous LL-37 had on the cellular expression of LL-37, IFN types I and II, IFN- β, and IFN-ϒ. The cellular (endogenous) expression of LL-37 remained the same at the 3 h time point for cells that were either only LL-37 treated or only infected. The cellular (endogenous) expression level of LL-37 changed, however, when cells were treated with LL-37 and infected (no pretreatment; Fig. 6). At 9 hpi, LL-37 treated cells, both uninfected and infected, remained relatively unchanged, with the exception of pretreated LL-

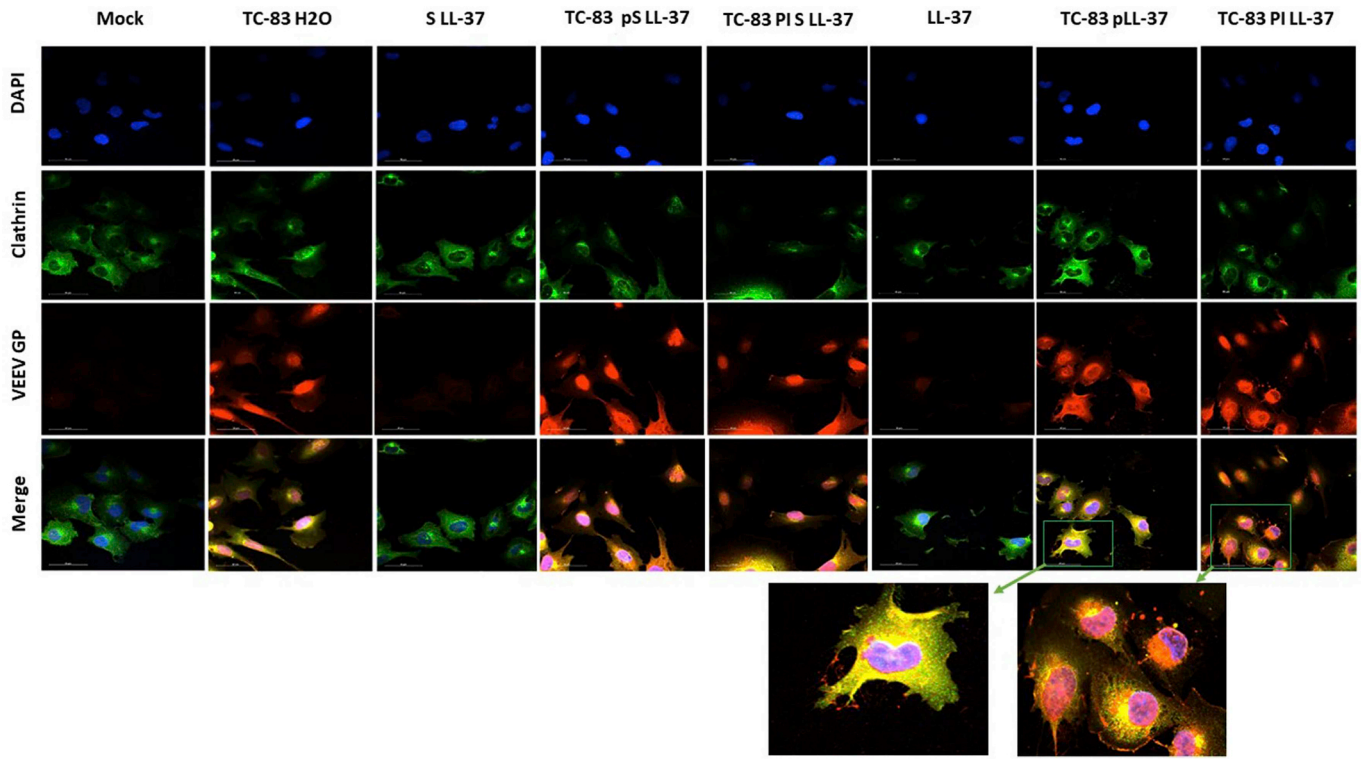

Fig. 4. Viral clumping in LL-37 treated cells. Confocal images showing the clumping of viruses as a result of LL-37 treatment. Magnified images of antibody to VEEV glycoprotein (red) show clumping of VEEV, which was not only extracellular but found throughout the cells. Nuclei are stained with DAPI (blue). Clathrin was used to visualize cells (green); VEEV glycoprotein is red. pLL-37 represents cells pre-treated with LL-37; PI LL-37 represents cells infected with TC-83 that was pre-incubated with LL-37. Scale bars in each case correspond to 50 μm.

37 cells (preLL-37), which demonstrated a modest increase in the levels of LL-37 expression (Fig. 6).

Although no change was evident in the expression of IFN-ϒ (data not shown), there was a noticeable increase in IFNβ1 expression as a result of TC-83 infection as compared to just LL-37 treatment. At 3 hpi, IFNβ1 expression was approximately 1-fold higher in TC-83-infected cells than in LL-37 treated, TC-83-infected cells. However, at 9 hpi, whereas TC-83-infected cells had about the same IFNβ1 expression as uninfected cells, LL-37-pretreated cells demonstrated a 6-fold increase in IFNβ1, and pre-incubated (pre-incLL-37) cells demonstrated a 4-fold increase in IFNβ1. These results indicate that LL-37 is a potent modulator of IFN- β expression.

4. Discussion

VEEV is a mosquito-transmitted virus that causes periodic outbreaks in many parts of the world. Previously weaponized, VEEV remains classified as a category B select agent (Hawley and Eitzen, 2001). In equines, VEEV infection results in high titer viremia, facilitating transmission to susceptible humans and other animals by mosquitoes. VEEV disease in humans is debilitating and occasionally fatal. Dissemination of VEEV in the central nervous system results in neuronal death and long-term neurological effects. During the course of encephalitic VEEV infection, infection-induced neuroinflammation disrupts BBB integrity thereby increasing permeability (Cain et al., 2017). So far, there is no treatment strategy that prevents viral replication and limits VEEV-induced neuroinflammatory events. Therefore, we investigated the possibility of applying the antimicrobial peptide LL-37, naturally produced in human cells by the expression of the CAMP gene, as an antiviral agent for VEEV.

In this study we determined that the host defense peptide LL-37 is a potent inhibitor of VEEV infection as well as a modulator of antiviral innate immune events. In our study, LL-37 demonstrated low toxicity and high antiviral activity against the VEEV derivative TC-83 in murine BV2 cells and in human HMC3 and U87MG cells. LL-37 inhibited viral replication in all three cell lines, thereby demonstrating generalized activity rather than cell-type dependency. LL-37 also inhibited the virulent TrD strain of VEEV as assessed with HMC3 cells.

It was expected that LL-37 would exert an inhibitory effect on VEEV as previous LL-37 antiviral activity against other types of virus was attributed to direct interaction with enveloped virions. LL-37 has been demonstrated to bind to and directly interact with the viral envelope proteins of DENV-2 (Alagarasu et al., 2017). In the case of vaccinia virus, an enveloped virus, pre-incubation with LL-37 alters the integrity of the viral membrane structure (Howell et al., 2004). Pre-incubation of HCV with LL-37 strongly inhibits the infectivity of this virus (Matsumura et al., 2016). While incubation of LL-37 with IAV drastically decreases viral replication, there is no apparent viral aggregation; however, virus-peptide interaction was observed and inhibitory activity of LL-37 was attributed to viral membrane degradation by LL-37 (Tripathi et al., 2013). Consistent with previously established and published results on the mechanism of action of LL-37, LL-37 pre-incubation with VEEV (specifically, with TC-83, an attenuated derivative) resulted in a more potent inhibitory response than treatment with LL-37 in the absence of pre-incubation.

We demonstrate that the antiviral activity of LL-37 is mediated, at least in part, by direct inhibition of the virus. Confocal microscopy revealed the presence of clustered viral material in LL-37-treated cells whereas virions were distributed throughout cells not treated with LL-37 (Fig. 4). The viral clusters appeared to be denser if TC-83 and LL-37 were pre-incubated prior to infection, supporting our hypothesis of direct inhibition of virus by the peptide. Electron microscopy further clarified the role LL-37 plays in VEEV inhibition. TEM images of virus-peptide interactions demonstrated extracellular as well as intracellular virion aggregation (Fig. 5). While the majority of viral clusters were extracellular, cytoplasmic clusters appeared to be located in vesicles.

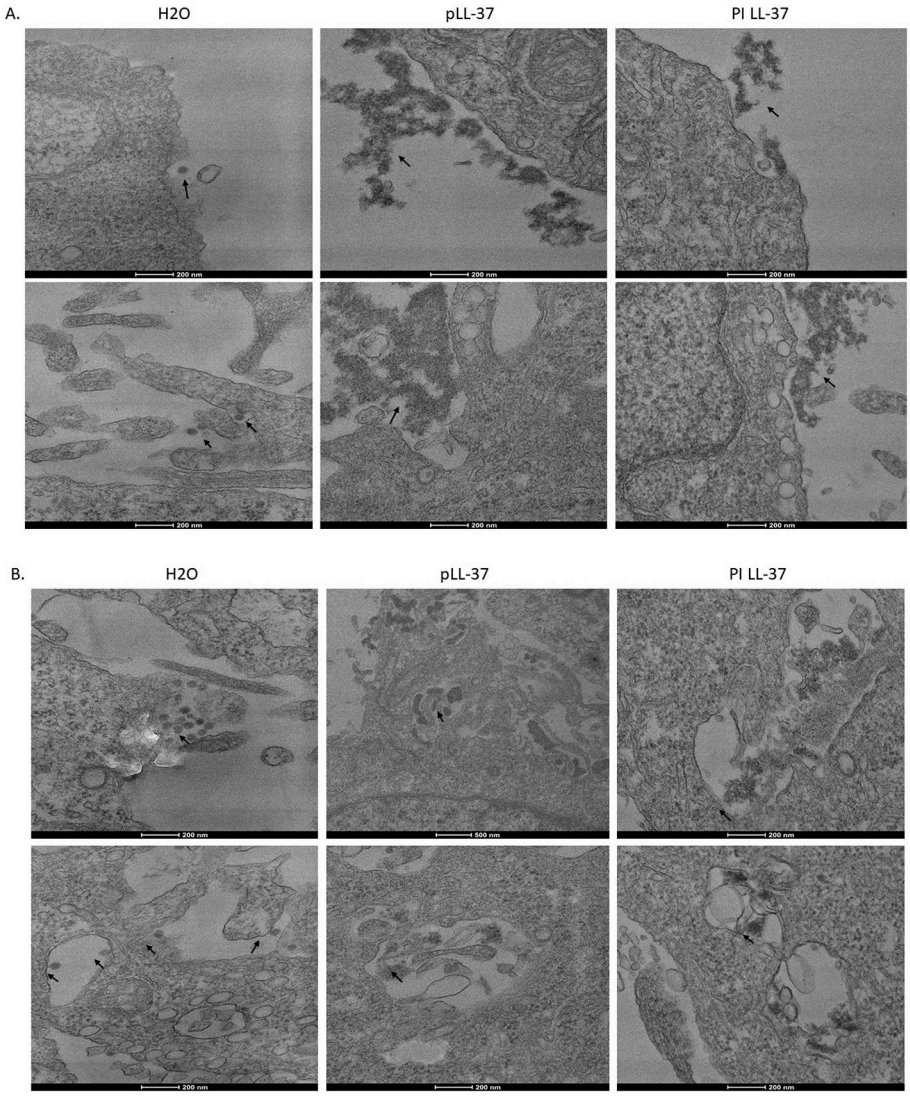

Fig. 5. TEM imaging showing TC-83 sequestered in clumps by LL-37, intracellularly and extracellularly. Cells were infected with TC-83 at an MOI of 5 for an hour and fixed at 3 hpi. (A) Extracellular TEM images show intact virus in the untreated panels (left, arrows) while clumping and aggregation of virions can be seen in the LL-37 treated panels (middle and right, arrows). (B) Sequestering of TC-83 in intracellular compartments can be seen in LL-37 treated cells (middle and right panels, arrows). In water-only treated cells, intact whole virions localized at the membranes of the compartments (arrows). pLL-37 represents cells pretreated with LL-37; PI LL-37 represents cells infected with TC-83 that was pre-incubated with LL-37.

This data supports the idea that the antiviral activity of LL-37 is mediated by its interaction with virions and, more specifically, by its interference with viral entry. If the interaction is one in which LL-37 penetrates the viral membrane or otherwise destroys its integrity, then these results correlate with a recent study demonstrating the LL-37 inhibition of Kaposi sarcoma-associated herpesvirus by viral membrane disruption (Brice et al., 2018).

Although the cell's endogenous expression of LL-37 is regulated during infection, various exogenous factors, such as inflammatory cytokines, can also affect it (Agier et al., 2015). While LL-37 mediated inhibition at early time points during infection, reduction in viral titers at 16 hpi indicate that there are other factors at play. We aimed to determine the effect of exogenous peptide on the expression of LL-37 upon stimulation with the peptide as a potential cellular activity that contributed to an antiviral state post-entry. Initially, at 3hpi, infection or LL-37 treatment alone did not have an effect on LL-37 expression. There was a significant decrease, however, in LL-37 mRNA levels in LL-37-treated samples and not as much of a decrease in the pretreatment conditions. This difference could possibly be attributed to the virus-peptide interactions/complexes that induce a change in endogenous LL-37 expression, as LL-37 mRNA levels decreased at later time points. Between the two time points, while LL-37 treated-infected samples remained relatively the same in terms of endogenous LL-37 expression, this expression decreased at 9 hpi in the non-infected and infected controls, which could be attributed to a possible LL-37 feedback mechanism or alternatively to a virus-mediated inhibition of endogenous LL-37 expression in the infected controls. Nonetheless, further investigation would allow the difference in LL-37 expression to be assessed more closely.

Interestingly, as expected, type I IFN expression drastically increased in infected cells treated with LL-37. While VEEV infection alone can elicit IFNβ1 expression, the expression of type I IFN increased 6-fold between 3 hpi and 9 hpi, for TC-83-infected cells stimulated by LL-37 resulting in an antiviral state. Whereas LL-37-treated cells demonstrated a significant increase in IFNβ1 expression, pretreated LL-37 samples demonstrated a less robust increase, which could possibly be due to lower initial internalization of LL-37, thus, less peptide available to induce a response. This slight decrease in IFNβ1 expression can also be explained in terms of the number of virions available to enter the cells and induce an antiviral response. IFNβ1 induces the activation of gene expression pathways that lead to an antiviral response (Levy and Garcia-Sastre, 2001). Further studies are required in order to determine the specific pathways and cytokines involved in controlling VEEV infection.

The results presented here demonstrate the efficacy of LL-37 as a potential therapeutic strategy to be developed for the treatment of VEEV infection. LL-37 acts directly on viral particles by inhibiting viral entry and exhibits indirect effects by modulating interferon expression and establishing an antiviral state. These data represent a novel and attractive basis for the future development of host defense peptides as

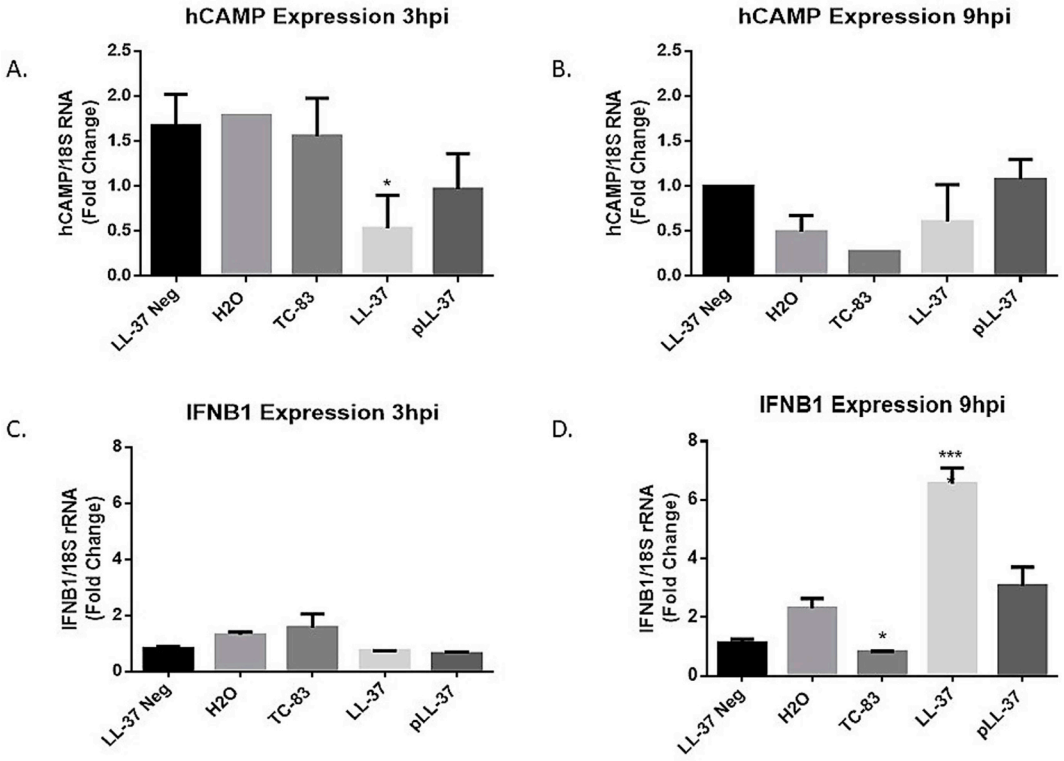

Fig. 6. Modulation of endogenous LL-37 and IFN expression as a result of exogenous LL-37. (A) Expression of hCAMP mRNA (CAMP encodes LL-37) at 3 hpi in the presence and absence of infection or LL-37 treatment. (B) hCAMP mRNA levels decreased in a time-dependent manner by at least 0.5 fold from 3 hpi to 9 hpi. (C) IFNβ1 expression levels were slightly higher in TC-83 infected cells without LL-37 treatment, as compared to IFNβ1 expression levels in cells treated with LL-37 at an early time point during the course of infection. (D) There was a significant increase in IFNβ1 mRNA levels at 9 hpi in LL-37 treated, TC-83 infected cells as compared to untreated TC-83 infected cells. pLL-37 represents cells pretreated with LL-37. Data reported as mean ± SD (n = 3). *p < 0.05, ***p < 0.001.

therapeutic strategies against alphavirus infections.

Author contributions

AA and AN designed the experiments. AA performed the experiments, wrote the manuscript and analyzed the data. GS, FK, SK, AB, and KR assisted with data collection. TL and CFN performed peptide design and provided peptide for initial testing. AN, AA, CFN and NB edited the manuscript. All authors read and approved the manuscript.

Competing financial interests

The authors declare that the research was conducted in the absence of any competing financial interests. TKL is a co-founder of Senti Biosciences, Synlogic, Engine Biosciences, Tango Therapeutics, Corvium, BiomX, and Eligo Biosciences. TKL also holds financial interests in nest. bio, Ampliphi, and IndieBio.

Acknowledgements

This work was funded through a Defense Threat Reduction Agency grant to AN. DTRA did not have any role in the design of the study, data analysis, or manuscript writing. We acknowledge support from the Ramon Areces Foundation (to CFN). Electron microscopy was performed at George Washington University Nanofabrication and Imaging Center under the direction and supervision of Dr. Christine Brantner.

Appendix A. Supplementary data

Supplementary data to this article can be found online at https://doi.org/10.1016/j.antiviral.2019.02.002.

References

Agier, J., Efenberger, M., Brzezinska-Blaszczyk, E., 2015. Cathelicidin impact on inflammatory cells. Cent. Eur. J. Immunol. 40, 225–235.
Alagarasu, K., Patil, P.S., Shil, P., Seervi, M., Kakade, M.B., Tillu, H., Salunke, A., 2017. In-vitro effect of human cathelicidin antimicrobial peptide LL-37 on dengue virus type 2. Peptides 92, 23–30.
Baer, A., Kehn-Hall, K., 2014. Viral concentration determination through plaque assays: using traditional and novel overlay systems. J. Vis. Exp., e52065.
Bahar, A.A., Ren, D., 2013. Antimicrobial peptides. Pharmaceuticals (Basel) 6, 1543–1575.
Barlow, P.G., Svoboda, P., Mackellar, A., Nash, A.A., York, I.A., Pohl, J., Davidson, D.J., Donis, R.O., 2011. Antiviral activity and increased host defense against influenza infection elicited by the human cathelicidin LL-37. PLoS One 6, e25333.
Bergman, P., Walter-Jallow, L., Broliden, K., Agerberth, B., Soderlund, J., 2007. The antimicrobial peptide LL-37 inhibits HIV-1 replication. Curr. HIV Res. 5, 410–415.
Brice, D.C., Toth, Z., Diamond, G., 2018. LL-37 disrupts the Kaposi's sarcoma-associated herpesvirus envelope and inhibits infection in oral epithelial cells. Antivir. Res. 158, 25–33.
Brown, K.L., Hancock, R.E., 2006. Cationic host defense (antimicrobial) peptides. Curr. Opin. Immunol. 18, 24–30.
Cain, M.D., Salimi, H., Gong, Y., Yang, L., Hamilton, S.L., Heffernan, J.R., Hou, J., Miller, M.J., Klein, R.S., 2017. Virus entry and replication in the brain precedes blood-brain barrier disruption during intranasal alphavirus infection. J. Neuroimmunol. 308, 118–130.
de la Fuente-Nunez, C., Mansour, S.C., Wang, Z., Jiang, L., Breidenstein, E.B., Elliott, M., Reffuveille, F., Speert, D.P., Reckseidler-Zenteno, S.L., Shen, Y., Haapasalo, M., Hancock, R.E., 2014. Anti-biofilm and immunomodulatory activities of peptides that inhibit biofilms formed by pathogens isolated from cystic fibrosis patients. Antibiotics (Basel) 3, 509–526.
Durr, U.H., Sudheendra, U.S., Ramamoorthy, A., 2006. LL-37, the only human member of the cathelicidin family of antimicrobial peptides. Biochim. Biophys. Acta 1758, 1408–1425.
Hawley, R.J., Eitzen Jr., E.M., 2001. Biological weapons–a primer for microbiologists. Annu. Rev. Microbiol. 55, 235–253.
He, M., Zhang, H., Li, Y., Wang, G., Tang, B., Zhao, J., Huang, Y., Zheng, J., 2018. Cathelicidin-derived antimicrobial peptides inhibit Zika virus through direct inactivation and interferon pathway. Front. Immunol. 9, 722.
Howell, M.D., Jones, J.F., Kisich, K.O., Streib, J.E., Gallo, R.L., Leung, D.Y., 2004. Selective killing of vaccinia virus by LL-37: implications for eczema vaccinatum. J. Immunol. 172, 1763–1767.

Julander, J.G., Skirpstunas, R., Siddharthan, V., Shafer, K., Hoopes, J.D., Smee, D.F., Morrey, J.D., 2008. C3H/HeN mouse model for the evaluation of antiviral agents for the treatment of Venezuelan equine encephalitis virus infection. Antivir. Res. 78, 230–241.

Kehn-Hall, K., Narayanan, A., Lundberg, L., Sampey, G., Pinkham, C., Guendel, I., Van Duyne, R., Senina, S., Schultz, K.L., Stavale, E., Aman, M.J., Bailey, C., Kashanchi, F., 2012. Modulation of GSK-3beta activity in Venezuelan equine encephalitis virus infection. PLoS One 7, e34761.

Kinney, R.M., Johnson, B.J., Welch, J.B., Tsuchiya, K.R., Trent, D.W., 1989. The full-length nucleotide sequences of the virulent Trinidad donkey strain of Venezuelan equine encephalitis virus and its attenuated vaccine derivative, strain TC-83. Virology 170, 19–30.

Levy, D.E., Garcia-Sastre, A., 2001. The virus battles: IFN induction of the antiviral state and mechanisms of viral evasion. Cytokine Growth Factor Rev. 12, 143–156.

Matsumura, T., Sugiyama, N., Murayama, A., Yamada, N., Shiina, M., Asabe, S., Wakita, T., Imawari, M., Kato, T., 2016. Antimicrobial peptide LL-37 attenuates infection of hepatitis C virus. Hepatol. Res. 46, 924–932.

Nijnik, A., Pistolic, J., Wyatt, A., Tam, S., Hancock, R.E., 2009. Human cathelicidin peptide LL-37 modulates the effects of IFN-gamma on APCs. J. Immunol. 183, 5788–5798.

Paessler, S., Weaver, S.C., 2009. Vaccines for Venezuelan equine encephalitis. Vaccine 27 (Suppl. 4), D80–D85.

Silva, O.N., de la Fuente-Nunez, C., Haney, E.F., Fensterseifer, I.C., Ribeiro, S.M., Porto, W.F., Brown, P., Faria-Junior, C., Rezende, T.M., Moreno, S.E., Lu, T.K., Hancock, R.E., Franco, O.L., 2016. An anti-infective synthetic peptide with dual antimicrobial and immunomodulatory activities. Sci. Rep. 6, 35465.

Steinstraesser, L., Tippler, B., Mertens, J., Lamme, E., Homann, H.H., Lehnhardt, M., Wildner, O., Steinau, H.U., Uberla, K., 2005. Inhibition of early steps in the lentiviral replication cycle by cathelicidin host defense peptides. Retrovirology 2, 2.

Strauss, J.H., Strauss, E.G., 1994. The alphaviruses: gene expression, replication, and evolution. Microbiol. Rev. 58, 491–562.

Tripathi, S., Tecle, T., Verma, A., Crouch, E., White, M., Hartshorn, K.L., 2013. The human cathelicidin LL-37 inhibits influenza A viruses through a mechanism distinct from that of surfactant protein D or defensins. J. Gen. Virol. 94, 40–49.

Weaver, S.C., Ferro, C., Barrera, R., Boshell, J., Navarro, J.C., 2004. Venezuelan equine encephalitis. Annu. Rev. Entomol. 49, 141–174.